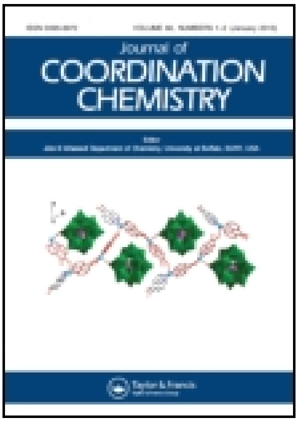

Journal of Coordination Chemistry
Publication details, including instructions for authors and subscription information:
http://www.tandfonline.com/loi/gcoo20

Thermotropic mesomorphism of mixed-valent diruthenium aliphatic carboxylates with axial anion bearing two aliphatic chains

Tamara Bottazzi[a], Florencia Cecchi[b], Andrés Zelcer[bd], Benoît Heinrich[c], Bertrand Donnio[c], Daniel Guillon[c] & Fabio D. Cukiernik[ab]

[a] Instituto de Ciencias, Universidad Nacional de General Sarmiento, Los Polvorines, Argentina

[b] INQUIMAE, Departamento de Química Inorgánica, Analítica y Química Física, Facultad de Ciencias Exactas y Naturales, Universidad de Buenos Aires, Ciudad Universitaria, Buenos Aires, Argentina

[c] Institut de Physique et Chimie des Matériaux de Strasbourg (IPCMS), Université de Strasbourg - CNRS, Strasbourg, France

[d] Gerencia Química, Centro Atómico Constituyentes, Comisión Nacional de Energía Atómica, Buenos Aires, Argentina

To cite this article: Tamara Bottazzi, Florencia Cecchi, Andrés Zelcer, Benoît Heinrich, Bertrand Donnio, Daniel Guillon & Fabio D. Cukiernik (2013) Thermotropic mesomorphism of mixed-valent diruthenium aliphatic carboxylates with axial anion bearing two aliphatic chains, Journal of Coordination Chemistry, 66:19, 3380-3390, DOI: 10.1080/00958972.2013.839783

To link to this article: http://dx.doi.org/10.1080/00958972.2013.839783

Journal of Coordination Chemistry, 2013
Vol. 66, No. 19, 3380–3390, http://dx.doi.org/10.1080/00958972.2013.839783

Thermotropic mesomorphism of mixed-valent diruthenium aliphatic carboxylates with axial anion bearing two aliphatic chains

TAMARA BOTTAZZI†, FLORENCIA CECCHI‡, ANDRÉS ZELCER‡¶, BENOÎT HEINRICH§, BERTRAND DONNIO§, DANIEL GUILLON§ and FABIO D. CUKIERNIK*†‡

†Instituto de Ciencias, Universidad Nacional de General Sarmiento, Los Polvorines, Argentina
‡INQUIMAE, Departamento de Química Inorgánica, Analítica y Química Física, Facultad de Ciencias Exactas y Naturales, Universidad de Buenos Aires, Ciudad Universitaria, Buenos Aires, Argentina
§Institut de Physique et Chimie des Matériaux de Strasbourg (IPCMS), Université de Strasbourg – CNRS, Strasbourg, France
¶Gerencia Química, Centro Atómico Constituyentes, Comisión Nacional de Energía Atómica, Buenos Aires, Argentina

(*Received 11 April 2013; accepted 7 August 2013*)

A homologous series of binuclear mixed-valent diruthenium tetracarboxylates, $Ru_2(O_2C(CH_2)_{n-2}CH_3)_4DHDP$ (DHDP = di(hexadecyl)phosphate axial anion, n = 10, 12, 14, 16, and 18), have been synthesized and characterized, and the liquid crystalline properties of these compounds were examined. All the compounds exhibit a room-temperature crystalline lamellar phase and a high temperature (above 140°) Col_h mesophase. Another, probably semi-crystalline, lamellar intermediate phase has also been found for all the studied compounds but for the n = 18 derivative. Comparison with related mesogenic homologous series where the equatorial ligands are also linear carboxylates, but the axial anions bear just one aliphatic chain (carboxylates, octylsulfonate, and dodecylsulfate), shows that the presence of a second aliphatic chain in the axial anion both lowers the transition temperatures and modifies the nature of the intermediate lamellar phase. Structural models at the molecular level are suggested for the crystalline lamellar and the Col_h phases.

Keywords: Coordination polymers; Ruthenium carboxylates; Metallomesogens; Columnar mesophases; Di(hexadecyl)phosphate

1. Introduction

Materials based on coordination compounds currently receive great attention due to the variety of physical properties expected to arise from the combination of their electronic structures and intermolecular organizations. A key aspect is to master the supramolecular

---

*Corresponding author. Email: fabioc@qi.fcen.uba.ar structure at a molecular level; in this context, metal-containing liquid crystals (called metallomesogens) provide a good example [1, 2]. The growth of research in the field of metallomesogens in the 1980s and 1990s arose from the enrichment of molecular geometries that coordination compounds could provide with respect to those observed in purely organic liquid crystals and the potential applications of the electrical, optical, and magnetic properties expected for coordination compounds in organized fluid media. Results in the first direction satisfied expectations; indeed, the extensive work carried out on coordination compounds involving ligands like substituted stilbazole, β-diketonates, Schiff-bases, phthalocyanines, carboxylates, among others, established firm correlations among molecular characteristics (type of ligand and nature of the central metal) and the structure of the liquid crystalline (LC) phases they can exhibit [1, 2]. The lack of significant advances in properties exploitation and applications prompted, a decade ago, some critical analysis of the research in the field [3] and a slight concomitant decrease in the research activities.

However, a renewed interest in both structural aspects (including supramolecular) [4–11] and physical properties [12–16] has emerged. As far as the molecular structure – type of mesophase relationship is concerned, the general trend is that nematic or smectic phases are usually found when Schiff bases, stilbazoles, or β-diketones are used as ligands (columnar mesophases have also been found when they carry several aliphatic chains), whereas metallophthalocyanines and bimetallic carboxylates usually have columnar mesophases.

In spite of their favorable structures, examples of coordination polymers (CPs) with columnar mesophases remain scarce [1, 2, 6, 12, 17]. The main reason is that usual bridging ligands are too long and create a void space between the mesogenic units which disfavors columnar mesomorphism. Indeed, the most studied mesogenic CPs are “shish-kebab” metallophthalocyanines [18–20], vanadyl-β-diketonates [21, 22], mixed-valent diruthenium tetracarboxylates ($Ru_2(O_2CR_{eq})_4X_{ax}$, scheme 1) [23–27], and iron-containing triazole derivatives [28, 29]. The first two types of compounds involve small axial ligands, like oxide or cyanide, bridging the essentially flat discotic units. In the third and fourth types of

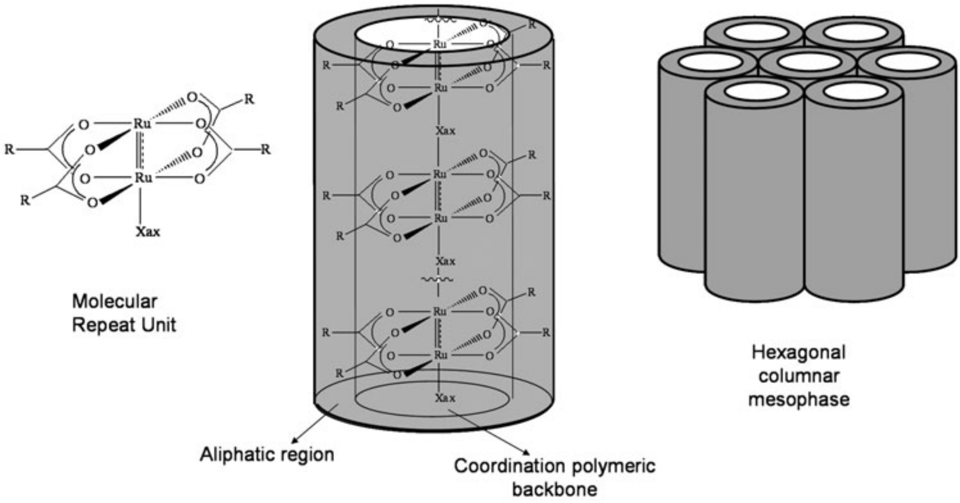

Scheme 1. Organization of coordination polymeric strands of mixed-valent diruthenium tertacarboxylates into hexagonal columnar mesophases.

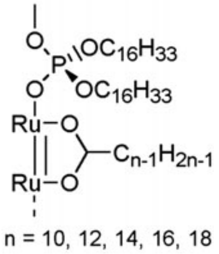

Scheme 2. Molecular formula of the repeat unit of the new mesogenic coordination polymers studied in this work.

compounds, the cores of the mesogenic units are slightly thicker, indeed no columnar mesomorphism has been found in mixed-valent diruthenium tetracarboxylates even for small axial anions, like chloride, if single aliphatic chains are equatorially attached [23, 24]. Our previous studies showed that efficient filling of the intermolecular space in an intracolumnar way is a successful strategy to columnar mesomorphism in $Ru_2(O_2CR_{eq})_4X_{ax}$ compounds, as it provides the necessary preorganization of the polymeric strands as parallel moieties in the crystalline phase [24, 26]. This has been achieved either with long chain axial anions (X_{ax}) [23–26] or equatorial R_{eq} substituents bearing several aliphatic chains, like di(alkoxy)- or tri(alkoxy)benzoates. This kind of equatorial filling of the space has also been used for columnar mesomorphism in the fourth type of compounds mentioned above – triazole-based derivatives – as well as in pyrazine-bridged diruthenium carboxylates [30]. Melting of the peripheral aliphatic chains during the crystalline to mesophase thermal transition transforms each CP into a column composed of a central polar core surrounded by an aliphatic region, as depicted in scheme 1; in turn, these columns organize in a hexagonal array. In some cases, more than one CP strand per column have been found [24, 26].

Among mesogenic diruthenium tetracarboxylates containing axial anions bearing one long aliphatic chain, compounds of general formula $Ru_2(O_2C(CH_2)_{n-2}CH_3)_4X_{lch}$, with X^-_{lch} = $CH_3(CH_2)_{n-2}CO_2^-$, $CH_3(CH_2)_{11}OSO_3^-$ (dodecylsulfate, DOS), or $CH_3(CH_2)_7SO_3^-$ (octylsulfonate, OS) axial anions, showed hexagonal columnar mesophases above 140–170 °C, depending on the equatorial chain length, n [23, 24, 26]. In this work, we extend those studies to a series containing an axial anion bearing two aliphatic chains, $Ru_2(O_2C(CH_2)_{n-2}CH_3)_4$DHDP (scheme 2, DHDP = di(hexadecyl)phosphate, $(C_{16}H_{31}O)_2PO_2^-$) for n = 10, 12, 14, 16, and 18. A molecular model consistent with the structural parameters is presented.

2. Experimental

$Ru_2(O_2C(CH_2)_{n-2}CH_3)_4$DHDP ($n$ = 10, 12, 14, 16, and 18) have been synthesized by metathesis reactions. 1.1 equivalents $AgNO_3$ dissolved in 10 mL methanol was added to a boiling solution of the corresponding $Ru_2(O_2C(CH_2)_{n-2}CH_3)_4Cl$ complex [24] (100 mg in 10–15 mL methanol). The precipitated AgCl was filtered off, then 1.2 equivalents potassium di(hexadecyl)phosphate (KDHDP) [31] dissolved in hot methanol was added to the mother liquor. After stirring under reflux for an hour, the solution was left to cool to room temperature. For n = 12, 14, 16, and 18, the pale brown precipitate was filtered, washed with cold methanol, and dried under vacuum. For the n = 10 derivative, water was added dropwise to the brown solution to complete precipitation; the fine precipitate thus obtained was filtered, washed with cold water–methanol mixture, and dried overnight under vacuum at 40 °C.

IR spectra were recorded as KBr pellets on a Nicolet FTIR 510P spectrometer. Diagnostic bands: 1490 (νCO_2assym), 1430 (δCH_2^{α}), 1420 (νCO_2sym) [32, 33], 1200 (νPO_4), and 1090 (νPO_4) cm^{-1} [34].

Elemental analyzes were carried out at *Servicio a Terceros* of INQUIMAE on a Carlo Erba CHNS-O EA1108 analyzer. Anal. Calcd for $Ru_2(O_2C(CH_2)_{16}CH_3)_4$DHDP (%): C, 66.4; H, 11.0. Found: C, 66.3; H, 10.9. Calcd for $Ru_2(O_2C(CH_2)_{14}CH_3)_4$DHDP (%): C, 65.2; H, 10.8. Found: C, 64.4; H, 10.9. Calcd for $Ru_2(O_2C(CH_2)_{12}CH_3)_4$DHDP (%): C, 63.8; H, 10.6. Found: C, 63.6; H, 11.3. Calcd for $Ru_2(O_2C(CH_2)_{10}CH_3)_4$DHDP (%): C, 62.2; H, 10.3. Found: C, 61.4; H, 10.4. Calcd for $Ru_2(O_2C(CH_2)_8CH_3)_4$DHDP (%): C, 60.3; H, 10.0. Found: C, 60.2; H, 10.0.

Mesomorphic properties have been studied by means of variable temperature polarizing optical microscopy (POM), differential scanning calorimetry (DSC), and variable temperature X-ray diffraction (XRD) techniques. POM has been carried out between crossed polarizers using a Leitz DMRX microscope equipped with a Leitz 1350 hot-stage. DSC experiments have been performed on a Shimadzu DSC-50 calorimeter. For the XRD experiments, powdered samples were contained in Lindemann capillaries of 1 mm diameter. A linear monochromatic Cu–Kα_1 beam (λ = 1.5418 Å) was obtained using a Debye-Scherrer camera, equipped with a bent quartz monochromator and an electric oven. Diffraction patterns (exposure time approx. 45 min) were registered every 10 °C, from 70 to 200 °C, with a gas curved counter "Inel CPS 120"; with this system, periodicities up to 60 Å can be measured, and the sample temperature is controlled within ± 0.05 °C.

3. Results

A simple two-step metathesis reaction has been employed for replacing the axial Cl^- by DHDP in the starting materials. Cl^- removal with Ag^+ allowed subsequent coordination of DHDP via methanolic bis-adducts as intermediates. The presence of DHDP in the final solids has been established on the basis of the presence of strong νPO_4 bands at 1200 and 1090 cm^{-1} in IR spectra of all of the synthesized compounds, which also exhibited typical bands associated with lantern-like diruthenium (II,III) tetracarboxylates [32, 33]. Microanalytical data confirmed the nature of the synthesized compounds.

All the compounds showed the same phase sequence: a room temperature crystalline lamellar phase (noted hereafter Cr) then a columnar hexagonal mesophase (Col$_h$) at temperatures higher than 135–145 °C. An intermediate phase has also been detected for the compounds except n = 18, which is discussed below. Table 1 collects the phase sequence and thermal parameters of each compound, as well as detailed information of their Col$_h$ mesophases. Figure 1 compares the XRD patterns obtained in the Col$_h$ mesophase for all the compounds under study. Representative DSC traces and XRD patterns for the low-temperature phases are given in figures S1 and S2, respectively. Detailed indexation of

Table 1. Phase sequence, thermal transition parameters and structural analysis of the Col_h mesophase for the $Ru_2(O_2C(CH_2)_{n-2}CH_3)_4$DHDP series.

	Phase sequences, transition temperatures (in °C) and transition enthalpies (in parenthesis, kJ/mol) for $Ru_2(O_2C(CH_2)_{n-2}CH_3)_4$DHDP. XRD data and refinement					
N	T/°C	d_{meas}/Å	hk	Intensity	d_{Calcd}/Å	Phase nature and structural parameters
Cr 127 (29) M 142 (2.8) Col_h 175 (−) I/dec						
10	150	22.23	10	VS (sh)	22.1	Col_h-$p6mm$
		12.66	11	M (sh)	12.75	$a = 25.5$ Å
		7.34	–	M (br)	h_2	$S = 563$ Å^2
		4.6	–	M (br)	h_{ch}	
		4.44	–	M (sh)	h_1	
Cr 122 (36) M 146 (4.7) Col_h 175 (−) I/dec						
12	150	22.98	10	VS (sh)	22.7	Col_h-$p6mm$
		13.17	11	M (sh)	13.1	$a = 26.2$ Å
		11.17	20	VW (sh)	11.35	$S = 595$ Å^2
		7.25	–	M (br)	h_2	
		4.7	–	M (br)	h_{ch}	
		4.47	–	M (sh)	h_1	
Cr 117 (36) M 137 (5.0) Col_h 180 (−) I/dec						
14	150	24.31	10	VS (sh)	24.15	Col_h-$p6mm$
		13.85	11	S (sh)	13.95	$a = 27.9$ Å
		12.08	20	W (sh)	12.1	$S = 674$ Å^2
		7.22	–	M (br)	h_2	
		4.6	–	M (br)	h_{ch}	
		4.48	–	M (br)	h_1	
Cr 122 (60) M 140 (3.0) Col_h 195 (−) I/dec						
16	170	24.89	10	VS (sh)	24.9	Col_h-$p6mm$
		14.47	11	S (sh)	14.4	$a = 28.75$ Å
		12.39	20	S (sh)	12.45	$S = 716$ Å^2
		7.18	–	M (br)	h_2	
		4.65	–	M (br)	h_{ch}	
		4.45	–	M (br)	h_1	
Cr 127 (76) M 138 (−) Col_h 185 (−) I/dec						
18	155	26.07	10	VS (sh)	25.95	Col_h-$p6mm$
		14.85	11	S (sh)	15.0	$a = 30.0$ Å
		13.03	20	S (sh)	13.0	$S = 777$ Å^2
		7.59	–	M (br)	h_2	
		4.55	–	M (br)	h_{ch}	
		4.42	–	M (br)	h_1	

XRD patterns for each compound in each phase at selected temperatures is presented in table S1.

The XRD patterns of the crystalline phase of the compounds are characterized (as shown in figure S2(a) for the $n = 16$ derivative) by several sharp peaks in the reciprocal ratio 1 : 2 : 3 : 4 : 5 : 6 : 7, etc.; narrow peaks at 7.4, 4.7, and 4.4 Å are also observed on every diffractogram. The presence of 3 or 4 broader peaks in the reciprocal ratio 1 : 2 : 3 in the XRD patterns of the intermediate phase, in addition to broad halos at *ca*. 7.5 and 4.7 Å and a weak narrow peak at 4.4 Å, as shown in figure S2(b) for $n = 14$ homolog, suggests that this intermediate phase possesses a lamellar morphology, with ordering reminiscent of the crystalline lamellar structure. In the high-temperature mesophase, all the compounds exhibited XRD patterns, shown in figure 1, with 3 peaks of decreasing intensity in the reciprocal ratio $1 : \sqrt{3} : \sqrt{4}$, corresponding to the 10, 11, and 20 reflections of a hexagonal array, broad peaks at *ca*. 7.5 Å and *ca*. 4.5 Å

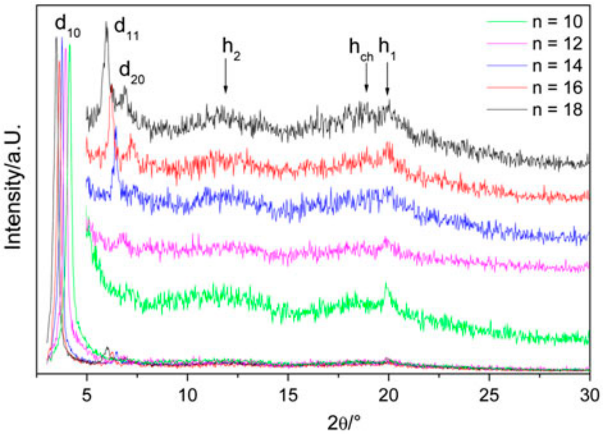

Figure 1. X-ray diffraction patterns of the $\mathrm{Col_h}$ mesophase for the $\mathrm{Ru_2(O_2C(CH_2)_{n-2}CH_3)_4DHDP}$ series (n = 10, 12, 14, 16, and 18).

(labeled on figure 1 as h_2 and h_{ch}, respectively), as well as a weak and narrower one at *ca*. 4.2 Å (h_1).

4. Discussion

The crystalline phase of this series of compounds is of the lamellar type, as already found for previously studied $\mathrm{Ru_2(O_2C(CH_2)_{n-2}CH_3)_4X_{\mathit{lch}}}$ series. The lamellar nature of this crystalline phase can be ascribed to the conformation of the equatorial aliphatic chains. Indeed, previous structural studies conducted on mid- and long-chain diruthenium (II,III) compounds [35, 36], as well as on divalent bimetallic carboxylates [37–39], found that two opposite aliphatic chains exhibit a gauche conformation at the C2–C3 bond, leading to elongated binuclear units in which the aliphatic chains run in parallel two by two. The total molecular length progressively increases by 2.54 Å per increment in n (number of carbons on each equatorial chain) [40, 41].

For mixed-valent $\mathrm{Ru_2(O_2CR)_4X_{\mathit{ax}}}$ compounds, the bimetallic units are axially linked by X_{ax}^-, giving “ribbons” with the CP backbone located at the center and the aliphatic chains pointing outwards. If the length of the axial chain (or chains in the case of DHDP) (l_{ax}) is similar to the length of the equatorial chains (l_{eq}), the CP backbones will be separated by a double layer of aliphatic chains as described in figure 2(a). In this structure, van der Waals interchain interactions reach their maximum value due to the interactions present inside each ribbon. On the other hand, if l_{ax} differs from l_{eq}, interdigitation can occur, providing additional van der Waals interactions between methylene/methyl units of adjacent ribbons, thus maximizing packing density (figure 2(b)). The distance between CP backbones, which is directly associated to the interlamellar distance d, varies with the number of carbon atoms in the equatorial chains (n) following expression (1):

$$d = w_{\mathrm{core}} + 2l_{\mathrm{CH_3}} + ((m-1) + (n-2))l_{\mathrm{CH_2}} \qquad (1)$$

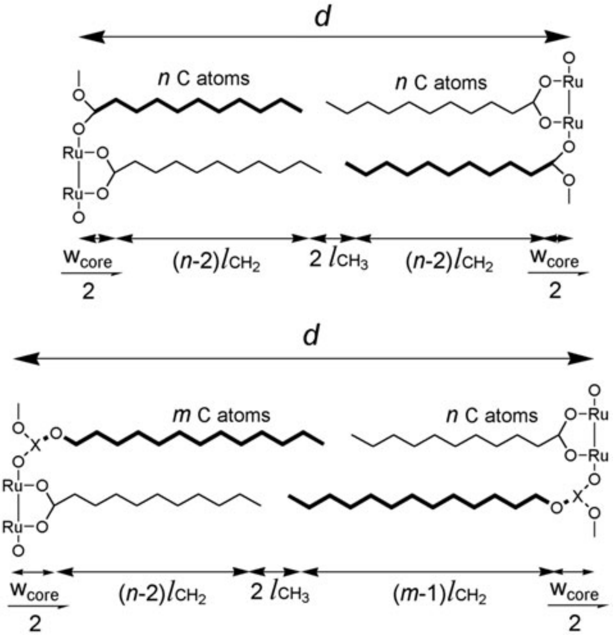

Figure 2. Schematic representation of the suggested model of molecular organization in the crystalline lamellar phase of $Ru_2(O_2C(CH_2)_{n-2}CH_3)_4X_{lch}$ compounds. (a) Upper scheme: compounds in which $l_{ax} = l_{eq}$, without interdigitation. A unitary increase in n should increase d in 2/CH_2 units. (b) Lower scheme: compounds in which $l_{ax} \approx l_{eq}$ including interdigitation.

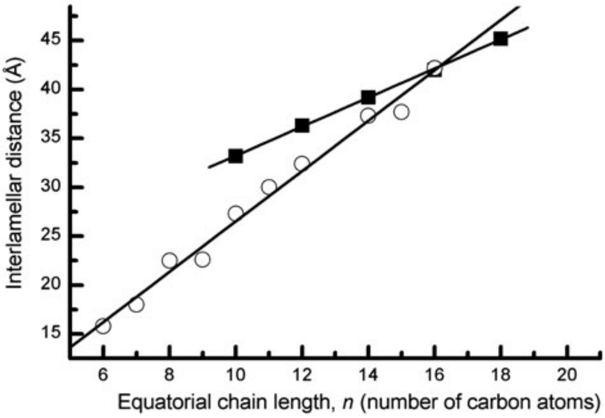

Figure 3. Interlamellar distance d as a function of the length of the equatorial chains, n, for the crystalline phase of the $Ru_2(O_2C(CH_2)_{n-2}CH_3)_4$DHDP series (filled squares). Data for $Ru_2(O_2C(CH_2)_{n-2}CH_3)_5$ series (open circles) also shown.

Figure 3 shows the interlamellar distances (d) found for the crystalline phase of the $Ru_2(O_2C(CH_2)_{n-2}CH_3)_4$DHDP series; the interlamellar distances previously found for the $Ru_2(O_2C(CH_2)_{n-2}CH_3)_5$ series [24] are also shown for comparison, corresponding to a situation in which $l_{ax} \cong l_{eq}$. As can be seen, d increases linearly with n in both cases, but the slope for the DHDP series (1.57 Å/CH_2) is about half that for the reference series (2.56 Å/CH_2), as expected for the suggested model (see Supplementary material for details). A similar situation has been found for previously studied OS and DOS series, for which interdigitation has also been suggested, although without detailed models like the one developed here.

It is easy to find, both on qualitative and quantitative bases (compare for example equations (1) and (S1)), that the interlamellar distance expected for an interdigitated structure should agree with that expected for a non-interdigitated one only when $l_{ax} \cong l_{eq}$; it is the case for DOS and OS [26] and for the present DHDP series (figure 3). This point also supports the assumption that, thanks to the tetrahedral geometry around P, the axial anion accommodates its aliphatic chains parallel among them as well as to the equatorial ones, acting in fact as a "wider" axial chain in an arrangement like the one found in the crystalline structure of $Ru_2(O_2C(CH_2)_8CH_3)_4OS$ [35].

An intermediate LC or semicrystalline Lam phase is a plausible intermediate state between lamellar Cr and Col_h phases. Indeed, intermediate lamellar phases have already been found between room temperature Cr lamellar phase and high temperature Col_h mesophase of related compounds [26]. However, in those cases, this intermediate lamellar phase is truly crystalline, whereas in the present case it is highly disordered, as evidenced by the collapse of the sharp reflections in almost the entire 2θ range and by the presence of the wide-angle halo characterizing the partially molten chains. This difference, established on the basis of both XRD and POM results, is in agreement with the low Lam → Col_h transition enthalpy (2–5 kJ/mol). The interlamellar distance is shorter than in the crystalline phase, possibly owing to a partial bending of the molten alkyl chains. The dependence of the interlamellar distance with n for the intermediate Lam phase is not easy to rationalize; moreover, it showed a strong dependence on temperature (see entries for $n = 16$ in table S1). Thus, we are not able to propose a structural model for this intermediate disordered Lam phase at the molecular level.

The high temperature mesophase is of the same type (Col_h) as the mesophase already found in previously studied $Ru_2(O_2C(CH_2)_{n-2}CH_3)_4X_{lch}$ series. The surface of the hexagonal unit cell increases linearly with n (figure 4), suggesting the presence of additional methylene units contributes just to the lateral expansion of the unit cell of the hexagonal

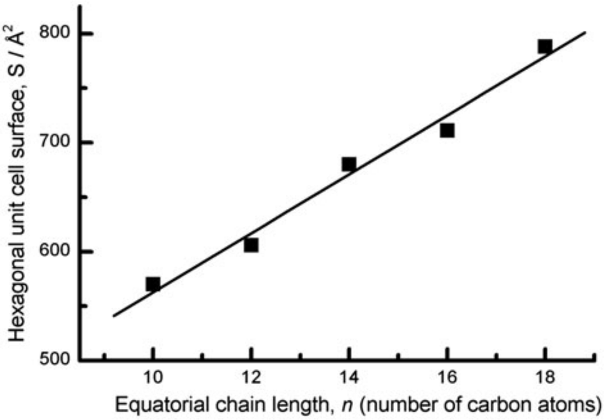

Figure 4. Surface of the hexagonal unit cell as a function of the length of the equatorial chains, n, for the Col_h mesophase of the $Ru_2(O_2C(CH_2)_{n-2}CH_3)_4DHDP$ series.

array, but not to modifications in the intracolumnar repeat distance, in agreement with the invariancy of h_2 position along the series (figure 1). This supports a model for the $\mathrm{Col_h}$ mesophase in which the central part of the column is occupied by the CP backbone, and the surrounding aliphatic chains are molten. In such a case, the slope of this straight line should be $p \times x \times \mathrm{V(CH_2)}/h$ (p: number of polymeric strands per column, x: number of aliphatic chains – per molecular unit – whose length varies along the series, $\mathrm{V(CH_2)}$: volume of a CH_2 group, and h: intracolumnar repeat distance) [24, 27, 42–44]. Assuming the halo at about 7.4 Å (labeled $\mathrm{h_2}$ in figure 1) corresponds to h (a value fully compatible with the repeat distance of a coordination polymeric strand with a slightly bent conformation, as found in $\mathrm{Ru_2(O_2C(CH_2)_8CH_3)_4OS}$) [35], and taking usual values for $\mathrm{V(CH_2)}$ in columnar or smectic mesophases [42, 45], the slope of this straight line (27.8 $\mathrm{Å^2/CH_2}$) shows that every column is made up of two coordination polymeric strands, suggesting that some degree of interdigitation between pairs of polymeric strands is still present. This was also the case for the other series in which $l_{ax} \neq l_{eq}$ (= DOS, OS) [26]. The weak peak detected at *ca*. 4.2 Å (labeled $\mathrm{h_1}$) superimposed to the broad one at approximately the same position could be interpreted as additional evidence for this suggestion. Indeed, if interdigitation is assumed for this $\mathrm{Col_h}$ mesophase, the interdigitated aliphatic chains will be located at the center of the column, and will exhibit much more constrained movements than the peripheral chains, expected to exhibit a liquid-like nature. The latter will originate the broad peak ($\mathrm{h_{ch}}$), whereas the former the weak and narrower one ($\mathrm{h_1}$).

5. Conclusions

The introduction of a second long aliphatic chain in the axial anion of the $\mathrm{Ru_2(O_2C(CH_2)_{\mathit{n}-2}CH_3)_4X_{\mathit{lch}}}$ family of compounds had two consequences on their mesomorphic behavior. The presence of this extra chain induces thermotropic polymorphism, in the form of a Lam – $\mathrm{Col_h}$ phase sequence for all but the longest homolog of the $\mathrm{Ru_2(O_2C(CH_2)_{\mathit{n}-2}CH_3)_4DHDP}$ series and it contributes to a substantial decrease in the melting temperatures. Indeed, the $\mathrm{Col_h}$ mesophase appears in the present case at temperatures lower than those found in structurally related systems with single alkyl chain sulfate, sulfonate, or carboxylate axial anions. Moreover, if melting temperatures to the intermediate phase are considered (Cr → Lam), the improvement in the width of the mesomorphic range is even greater. Combined to its high clearing temperatures, these thermal features yield the $\mathrm{Ru_2(O_2C(CH_2)_{\mathit{n}-2}CH_3)_4DHDP}$ series one of the $\mathrm{Ru_2(O_2C(CH_2)_{\mathit{n}-2}CH_3)_4X_{\mathit{lch}}}$ family exhibiting the widest mesomorphic thermal range. These findings add new insights to understand the influence that different ligands can exert on the structural organization of CPs and subsequently on some of their physical properties, including mesomorphism.

Supplementary material

Representative DSC traces and XRD patterns, detailed XRD information for each compound in each phase as well as a more detailed analysis of the struture of the crystalline lamellar phase can be found as supplementary material.

Acknowledgments

We thank Martin Gaitan for his help to TB during the synthesis of most of the reported compounds. Financial support from UBACyT (X219 and X057) and ANPCyT (PICT25409) is acknowledged. TB thanks UNGS for a research fellowship, FC thanks CONICET for a PhD research fellowship. FDC and AZ are members of the research staff of Conicet. BD, BH, and DG thank CNRS and Université de Strasbourg for their support.

References

[1] J.L. Serrano (Ed.). *Metallomesogens*, VCH, Weinheim (1996).

[2] B. Donnio, D. Guillon, R. Deschenaux, D.W. Bruce. In *Comprehensive Coordination Chemistry*, J. McCleverty, T.J. Meyer (Eds), Vol. 7, pp. 357–627, Elsevier Pergamon, Amsterdam (2004).

[3] R. Gimenez, D.P. Lydon, J.L. Serrano. *Curr. Opin. Sol. State Mater. Sci.*, **6**, 527 (2002).

[4] C.R. Bhattacharjee, G. Das, P. Mondal. *J. Coord. Chem.*, **64**, 3273 (2011).

[5] C.R. Bhattacharjee, G. Das, D.D. Purkayastha, P. Kanoo, P. Mondal. *J. Coord. Chem.*, **64**, 2746 (2011).

[6] M. Seredyuk, A.B. Gaspar, V. Ksenofontov, Y. Galyametdinov, M. Verdaguer, F. Villain, P. Gütlich. *Inorg. Chem.*, **47**, 10232 (2008).

[7] K. Nejati, Z. Rezvani, E. Alizadeh, R. Sammimi. *J. Coord. Chem.*, **64**, 1859 (2011).

[8] P.W. Shakya, A.K. Singh, T.R. Rao. *J. Coord. Chem.*, **65**, 3519 (2012).

[9] Y. Molard, F. Dorson, V. Cîrcu, T. Roisnel, F. Artzner, S. Cordier. *Angew. Chem. Int. Ed.*, **49**, 3351 (2010).

[10] M.A. Castro, A.E. Roitberg, F.D. Cukiernik. *J. Comput. Chem.*, **34**, 1283 (2013).

[11] T. Cardinael, J. Ramaekers, K. Driesen, P. Nockemann, K. Van Hecke, L. Van Meervelt, B. Goderis, K. Binnemans. *Inorg. Chem.*, **48**, 2490 (2009).

[12] J. Barberá, I. Lantero, S. Moyano, J.L. Serrano, A. Elduque, R. Giménez. *Chem. Eur. J.*, **16**, 14545 (2010).

[13] M.A. Castro, A.E. Roitberg, F.D. Cukiernik. *J. Chem. Theory Comput.*, **9**, 2609 (2013).

[14] P. Grondin, D. Siretanu, O. Roubeau, M.-F. Achard. R. Clérac, *Inorg. Chem.*, **51**, 5417 (2012).

[15] Y. Bodenthin, G. Schwarz, Z. Tomkowicz, T. Geue, W. Haase, U. Pietsch, D.G. Kurth. *J. Am. Chem. Soc.*, **131**, 2934 (2009).

[16] E. Terazzi, C. Bourgogne, R. Welter, J.L. Gallani, D. Guillon, G. Rogez, B. Donnio. *Angew. Chem. Int. Ed.*, **47**, 490 (2008).

[17] L. Oriol. In *Metallomesogens*, J.L. Serrano (Ed.), pp. 193–231, VCH, Weinheim (1996).

[18] M. Hanack, A. Beck, H. Lehmann. *Synthesis*, 703 (1987).

[19] A.P.M. Kentgens, B.A. Markies, J.F. Van der Pol, R.J.M. Nolte. *J. Am. Chem. Soc.*, **112**, 8800 (1990).

[20] T. Sauer. *Macromolecules*, **26**, 2057 (1993).

[21] W. Haase, D. Kilian, M.A. Athanassopoulou, D. Knawby, T.M. Swager, S. Wrobel. *Liq. Cryst.*, **29**, 133 (2002).

[22] H. Zheng, C.K. Lai, T.M. Swager. *Chem. Mater.*, **7**, 2067 (1995).

[23] F.D. Cukiernik, P. Maldivi, A.M. Giroud-Godquin, J.C. Marchon, M. Ibn-Elhaj, D. Guillon, A. Skoulios. *Liq. Cryst.*, **9**, 903 (1991).

[24] F.D. Cukiernik, M. Ibn-Elhaj, Z. Chaia, J.C. Marchon, A.M. Giroud-Godquin, D. Guillon, A. Skoulios, P. Maldivi. *Chem. Mater.*, **10**, 83 (1998).

[25] J.F. Caplan, C.A. Murphy, S. Swansburg, R.P. Lemieux, T.S. Cameron, M.A.S. Aquino. *Can. J. Chem.*, **76**, 1520 (1998).

[26] Z. Chaia, A. Zelcer, B. Donnio, M. Rusjan, F.D. Cukiernik, D. Guillon. *Liq. Cryst.*, **31**, 1019 (2004).

[27] Z. Chaia, M. Rusjan, M.A. Castro, B. Donnio, B. Heinrich, D. Guillon, R. Baggio, F.D. Cukiernik. *J. Mater. Chem.*, **19**, 4981 (2009).

[28] M. Seredyuk, A.B. Gaspar, V. Ksenofontov, S. Reiman, Y. Galyametdinov, W. Haase, E. Rentschler, P. Gütlich. *Chem. Mater.*, **18**, 2513 (2006).

[29] T. Fujigaya, D.-L. Jiand, T. Aida. *J. Am. Chem. Soc.*, **127**, 5484 (2005).

[30] M. Rusjan, B. Donnio, D. Guillon, F.D. Cukiernik. *Chem. Mater.*, **14**, 1564 (2002).

[31] C.M. Paleos, D. Kardassi, D. Tsiourvas, A. Skoulios. *Liq. Cryst.*, **25**, 267 (1998).

[32] Z.D. Chaia. Sintesis y Estudios Ficoquimicos de CRistales Liquidos Moleculares Derivados de Rutenio y Cobre [Synthesis and physicochemical studies on ruthenium and copper based molecular liquid crystals] PhD thesis, University of Buenos Aires (2002).

[33] M.A.S. Aquino. *Coord. Chem. Rev.*, **170**, 141 (1998).

[34] K. Nakamoto. *Infrared and Raman Spectra of Inorganic and Coordination Compounds*, 4th Edn, John Wiley, New York (1986).

[35] A. Zelcer, Z. Chaia, F.D. Cukiernik, E.E. Castellano, O.E. Piro. *Acta Cryst.*, **C58**, m144 (2002).

[36] F.D. Cukiernik, J.C. Marchon, D. Luneau, P. Maldivi. *Inorg. Chem.*, **37**, 3698 (1998).

[37] T.R. Lomer, K. Perera. *Acta Cryst.*, **B30**, 2912 (1974).

[38] F.A. Cotton, K.B. Shiu. *Rev. Chim. Miner.*, **23**, 14 (1986).

[39] G.C. Campbell, J.F. Haw. *Inorg. Chem.*, **27**, 3706 (1988).

[40] H. Abied, D. Guillon, A. Skoulios, P. Weber, A.M. Giroud-Godquin, J.C. Marchon. *Liq. Cryst.*, **2**, 269 (1987).

[41] D.V. Baxter, R.H. Cayton, M.H. Chisholm, J.C. Huffman, E.F. Putilina, S.L. Tagg, J.L. Wesemann, J.W. Zwanziger, F.D. Darrington. *J. Am. Chem. Soc.*, **116**, 4551 (1994).

[42] T. Sauer, G. Wegner. *Mol. Cryst. Liq. Cryst.*, **162B**, 97 (1988).

[43] D. Guillon. *Struct. Bond. (Berlin)*, **95**, 42 (1999).

[44] A.M. Levelut. *J. Chim. Phys.*, **80**, 149 (1983).

[45] D. Guillon, A. Skoulios, J.J. Benattar. *J. Phys.*, **47**, 133 (1986).